Research

The climate envelope of Alaska's northern treelines: implications for controlling factors and future treeline advance

Colin T. Maher, Roman J. Dial, Neal J. Pastick, Rebecca E. Hewitt, M. Torre Jorgenson and Patrick F. Sullivan

C. T. Maher (https://orcid.org/0000-0001-8409-7775)

(ctmaher@alaska.edu) and P. F. Sullivan (https://orcid.org/0000-0002-8015-3036), Environment and Natural Resources Inst., Univ. of Alaska, Anchorage, AK, USA. – R. J. Dial, Inst. of Culture and Environment, Alaska Pacific Univ., Anchorage, AK, USA. – N. I. Pastick, KBR Inc., contractor to the U.S. Geological Survey, Earth Resources and Observation Science Center, Sioux Falls, SD, USA. – R. E. Hewitt, Center for Ecosystem Science and Society, Northern Arizona Univ., Flagstaff, AZ, USA and Dept of Environmental Studies, Amherst College, Amherst, MA, USA. – M. T. Jorgenson, Alaska Ecoscience, Fairbanks, AK, USA.

Ecography 44: 1-13, 2021 doi: 10.1111/ecog.05597

Subject Editor and Editor-in-Chief: Jens-Christian C Svenning Accepted 3 August 2021



Understanding the key mechanisms that control northern treelines is important to accurately predict biome shifts and terrestrial feedbacks to climate. At a global scale, it has long been observed that elevational and latitudinal treelines occur at similar mean growing season air temperature (GSAT) isotherms, inspiring the growth limitation hypothesis (GLH) that cold GSAT limits aboveground growth of treeline trees, with mean treeline GSAT ~6-7°C. Treelines with mean GSAT warmer than 6-7°C may indicate other limiting factors. Many treelines globally are not advancing despite warming, and other climate variables are rarely considered at broad scales. Our goals were to test whether current boreal treelines in northern Alaska correspond with the GLH isotherm, determine which environmental factors are most predictive of treeline presence, and identify areas beyond the current treeline where advance is most likely. We digitized ~12 400 km of treelines (>26 K points) and computed seasonal climate variables across northern Alaska. We then built a generalized additive model predicting treeline presence to identify key factors determining treeline. Two metrics of mean GSAT at Alaska's northern treelines were consistently warmer than the 6-7°C isotherm (means of 8.5°C and 9.3°C), indicating that direct physiological limitation from low GSAT is unlikely to explain the position of treelines in northern Alaska. Our final model included cumulative growing degree-days, near-surface (≤1 m) permafrost probability and growing season total precipitation, which together may represent the importance of soil temperature. Our results indicate that mean GSAT may not be the primary driver of treeline in northern Alaska or that its effect is mediated by other more proximate, and possibly non-climatic, controls. Our model predicts treeline potential in several areas beyond current treelines, pointing to possible routes of treeline advance if unconstrained by non-climatic factors.

Keywords: boreal forest, growth limitation hypothesis, permafrost, tundra-taiga ecotone



www.ecography.org

Introduction

Treelines - the widespread vegetation boundaries between forest and tundra - have interested scientists for over a century (Gannett 1899, Daubenmire 1954, Tuhkanen 1993, Körner 2012, Holtmeier and Broll 2020). The potential of treelines as bellwethers of climate change has inspired new efforts to understand these boundaries (Bader et al. 2020). Understanding how, where and when treelines form is challenging because potential driving factors are confounded; biophysical attributes co-vary and are interrelated along the environmental gradients that characterize forest-tundra ecotones. In addition, treelines are variable in structure, composition and geographic position and can be difficult to access, which limits opportunities for experimental studies of generalizable causal factors. Nevertheless, understanding the relative importance of the causes of treelines has implications for species range limits (Risser 1995), carbon cycling (Wilmking et al. 2006), broad-scale atmospheric circulation patterns (Pielke and Vidale 1995) and surface energy balance (Chapin et al. 2005). Understanding controls on treelines between the vast boreal forest and tundra biomes of Eurasia and North America is especially important because advancing forest could amplify current warming trends.

The strong correlation of latitudinal and elevational treelines with temperature was noted by early researchers, along with the hypothesis that cool growing season air temperature is the primary cause of treelines (Gannett 1899, Daubenmire 1954). Further explaining this association, Körner (1998) advanced the 'growth limitation hypothesis' (GLH). The GLH posits that aerodynamic coupling of tallstatured trees with cold air - and the resultant constraints on cell division - is the ultimate reason trees fail to grow above certain elevations or latitudes globally (Körner 1998, 2012, Körner and Paulsen 2004). Observational elaborations of the GLH identified global treeline mean growing season air temperatures (GSATs) as 6.7°C (Körner and Paulsen 2004) and 6.4°C (Körner 2012, Paulsen and Körner 2014). Mean GSATs of 6-7°C are plausible if trees near treelines are primarily growth-limited; the critical daily minimum air temperature at the onset and cessation of wood formation (xylogenesis) in conifers was estimated to be 4-5°C (daily means of 8-9°C; Rossi et al. 2008) and as low as ~0.7°C at treeline (daily means of ~3.9°C; Li et al. 2017).

The specific mechanisms of the GLH allow a conceptually simple test: if the GLH explains treelines globally, then examinations of mean GSAT at many treelines should reveal values centered on 6–7°C. Körner and Paulsen's (2004) analysis of soil temperature did find that subarctic and boreal treelines match an isotherm between 6 and 7°C (global mean \pm SD of 6.7 \pm 0.8°C), but their sample of northern treelines was small (three sites), and the authors used seasonal mean soil temperature to estimate mean GSAT. Although this method may be accurate at lower latitudes, mean seasonal soil temperature at boreal treelines can be much colder than GSAT due to permafrost and associated high soil water content (Romanovsky and Osterkamp 2000, Sullivan et al. 2015). More extensive

sampling of treelines is needed, particularly in boreal regions, to assess their climatic attributes and to understand their causal factors. Because only slightly more than half of all treelines studied globally have advanced in response to anthropogenic warming (Harsch et al. 2009), there is a clear need to consider environmental variables other than GSAT at broad scales.

Our objectives were to evaluate the correspondence of treelines in northern Alaska with the mean GSAT isotherm specified by the GLH, determine which environmental factors best predict treeline presence, and identify areas currently beyond the treeline with climates that could support treeline expansion. Similar to species distribution modelling, we determined which environmental factors are likely correlated with treeline presence. We then applied a hypothetico-deductive framework to test the temperature isotherm aspect of the GLH: if Alaska's boreal treeline position is limited by cold GSAT, 1) mean GSAT at treelines will be centered around 6–7°C and 2) metrics of GSAT will be the most important predictors of treeline presence. Finally, we mapped model predictions over northern Alaska to determine specific areas that may currently be climatically suitable for treeline advance.

Our specific research questions were:

- 1) Do boreal treelines across northern Alaska fall within the 6–7°C mean GSAT isotherm associated with the growth limitation hypothesis?
- 2) Which variables make the best predictive model of treeline presence in northern Alaska and how well does the model predict treelines?
- 3) Based on model predictions, where will treelines most likely expand in northern Alaska?

Methods

Study area

Our study area was all of the U.S. state of Alaska north of 66°N (northern Alaska), where boreal lowlands in Alaska's interior region are separated from the North Slope by the ~1000 km Brooks Range. White spruce *Picea glauca* is the dominant treeline species throughout the Brooks Range and in much of northern Alaska, although black spruce *Picea mariana* can also form treelines (Viereck and Little 2007). Elevational treelines in northern Alaska are rarely bounded by upper shrublines of *Alnus*, *Salix* or *Betula* that separate forest from alpine tundra, unlike elsewhere in Alaska (Dial et al. 2016). Permafrost is present throughout the region, at least discontinuously, and is most widespread and continuous on the North Slope. However, permafrost degradation is occurring and is expected to accelerate in the coming decades (Pastick et al. 2015).

Treeline presence/absence dataset and sampling

We used a previously published coarse-scale Alaska treeline (Jorgenson and Meidinger 2015; JM) to guide a detailed and

extensive treeline digitization effort. The JM treeline delineates broad regions of forest and tundra, as determined from Landsat imagery, but does not correspond precisely to local tree limits, which are not usually visible at 30 m pixel resolution. Furthermore, because the JM treeline is meant to qualitatively separate boreal forest from tundra, the line frequently bridges gaps between forest patches where there are no trees. We used very high resolution (<1 m pixels), cloud-free imagery available on Google Earth™ or archived at EVWHS (<https://evwhs.digitalglobe.com>) such as Quickbird and WorldView to refine the JM treeline (Supporting information). For the purposes of identification, we defined treelines inclusively as ecotones between areas containing some visible trees and areas with no visible trees. These included, but were not exclusive to, treelines on hillslopes (generally considered alpine treelines) and in lowlands (often considered latitudinal or boreal treelines). We digitized treelines as the outer edge of tree occurrence, without stipulating they be single connected lines.

Unable to manually digitize all treelines throughout our study area, we strove to establish that non-treeline points (i.e. absences) were correctly classified in the dataset used in model building and assessment. We thus generated 65 sample disks (10 km radius), both as a grid (n=45) and along the northernmost treeline (n=20), to ensure a representative sample of the range of treeline locations in northern Alaska (Fig. 1). We examined imagery within each of the disks and digitized all treelines, if present. After treelines were digitized, we imported the lines into R ver. 4 (<www.r-project.org>) and converted them to a raster grid with a 0.00833° resolution (337 × 918 m with Albers Equal Area projection; Supporting information). Each pixel crossed by a treeline was coded as treeline-present (1). All other pixels were coded as treeline-absent (0). The total length of all treelines recorded was ~12 400 km (26 209 pixels; Fig. 1). The final sample dataset consisted of all pixels within sampling disks for a total of 61 441 observations (8357 treeline-present, 53 084 treeline-absent).

Environmental variable dataset

We assembled raster maps of seasonal climatic variables for northern Alaska from several source datasets: modelled/interpolated monthly 2 m air temperature and precipitation normals (1981–2010) from PRISM (Daly et al. 2008), observed daily snow cover for 2006–2019 from the National Snow and Ice Data Center (U.S. National Ice Center 2008,

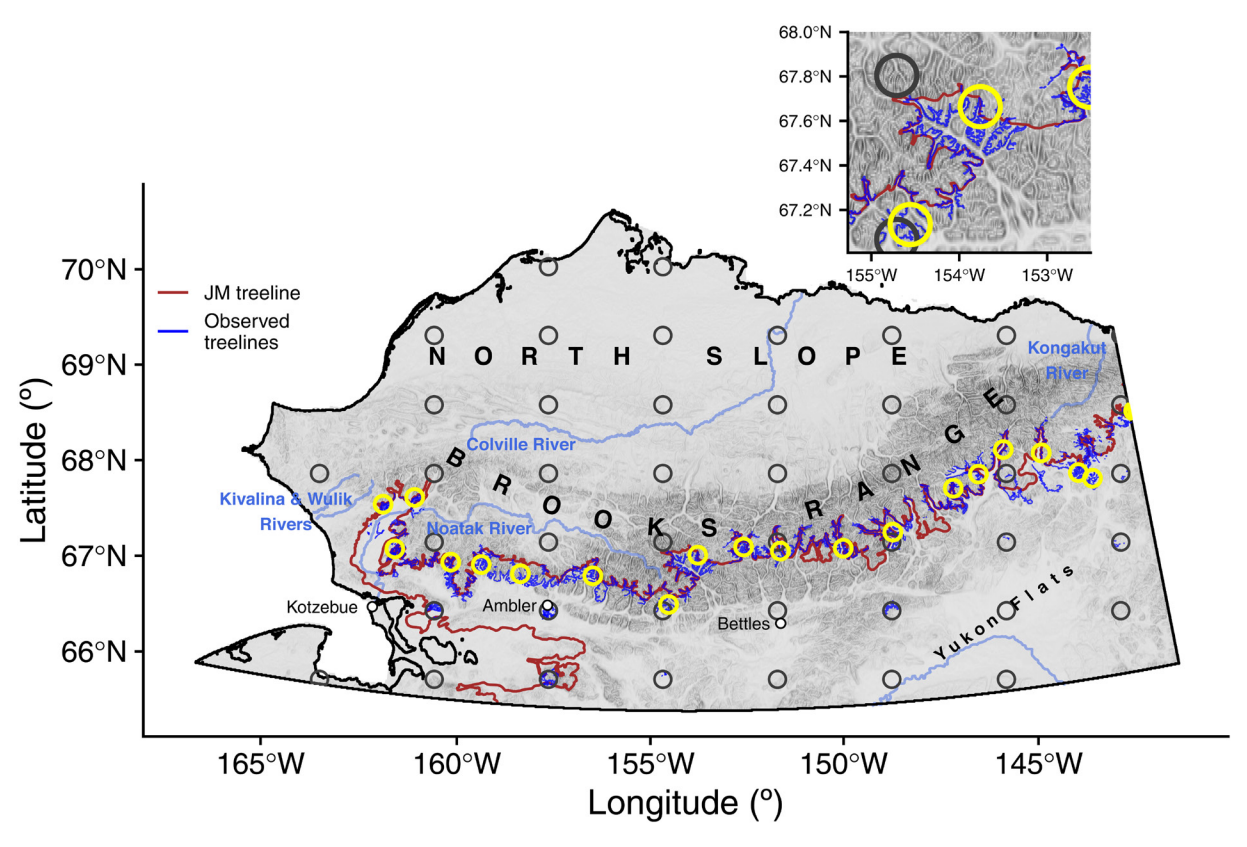


Figure 1. Layout of the sampling design in northern Alaska. We used high resolution satellite imagery to digitize all observable treelines (dark blue lines) in the Brooks Range mountains using the general Jorgenson and Meidinger (2015; brown line) treeline as a guide (inset map shows distinction in detail). We then selected a systematic sample of 10 km radius disks in a string along our observed treelines (n = 20; yellow circles) and in a systematic grid across the landscape (n = 45; dark gray circles). We examined imagery in each disk and digitized any additional treelines we identified within. Finally, treeline presence and environmental variables were extracted for all pixels inside each disk to create the sample dataset used for model training and validation.

updated daily), and modelled/interpolated monthly 10 m wind normals (1981–2010) from the TerraClimate dataset (Abatzoglou et al. 2018). We used the native PRISM resolution (0.00833°, 337 \times 918 m) for all analysis, re-scaling other datasets where necessary using the nearest neighbour method (Table 1). To approximate seasons with daily resolution in each pixel, we applied the methods of Paulsen and Körner (2014) by transforming monthly normals into pseudo-daily data using smoothing splines through monthly values. Interpreted as pseudo-daily values, monthly means represent values near the 15th day.

We defined growing, fall, winter and spring seasons for each pixel in the landscape. We defined tree-specific growing seasons as all days with a daily mean air temperature greater ≥ 4°C (the seasonal base temperature), informed by published seasonal temperature thresholds for onset and cessation of xylogenesis (Rossi et al. 2008, Li et al. 2017). We further constrained growing seasons by subtracting days before the median first snow-free date for each pixel, when snow persisted after daily means exceeded the base temperature (as in Paulsen and Körner 2014). We defined fall as daily means ≤ 4° C, but with daily maximum temperatures $\geq 0^{\circ}$ C. Winter included all days with daily maximum < 0°C. Spring was defined as daily maximum $\geq 0^{\circ}$ C and before the growing season (either the 4°C mean daily base temperature or the first snow-free day). Although the 4°C mean daily base defined growing seasons for most variables, we also calculated cumulative growing degree-days with other temperature bases (0, 4 and 5°C) to test the relevance of heat sums for treeline presence. Growing degree-days were calculated as the sum of temperatures for all days above the temperature base (Man and Lu 2010), ignoring snow cover. We performed most

calculations using the raster package (Hijmans 2021) in R ver. 4 (<www.r-project.org>).

While historical estimates of active-layer depth and permafrost conditions are available in Alaska (Pastick et al. 2017). past model simulations relied on vegetation characteristics that could confound our analysis. Therefore, we developed a map (90 m resolution) of near-surface permafrost probabilities using field observations, permafrost-related topographic data and the machine learning framework of Pastick et al. (2015), excluding Landsat imagery and land cover data. This consisted of 1) extracting environmental data: average annual and seasonal temperature (Hijmans et al. 2005), monthly snow cover fractions (Hall et al. 2016), soil organic carbon (Wylie et al. 2016) and interferometric synthetic aperture radar (IFSAR)-derived topographic metrics at each field site; 2) randomly splitting (90/10) this database for random forest model training and validation (Breiman 2001); 3) selecting optimal hyper-parameters using the random search method (Bergstra and Bengio 2012); and 4) applying the classification model in Google Earth Engine (Gorelick et al. 2017). Our independent accuracy assessment and reliability plots revealed good agreement between mapped and observed values across Alaska (area under the receiver operating characteristic curve [AUC] = 0.93). The resulting data represent simulated probabilities of encountering permafrost within 1 m of the ground surface.

Testing the 6-7°C isotherm associated with the GLH

To investigate mean GSAT at treeline, we created two raster layers using the pseudo-daily temperature data. One layer used the 4°C base temperature corresponding with

Table 1. Descriptions of explanatory environmental variables used for building models predicting treeline presence in northern Alaska. There were 48 variables in total. Seasonal abbreviations are as follows: GS=growing season, SP=spring, FA=fall and WI=winter.

Variable	Description	Units	Time periods covered	Native resolution
FAL	Length of the fall season. Period between tmean $< 4^{\circ}\text{C}$ and tmax $< 0^{\circ}\text{C}$.	Days	Annual	800 m
Frost risk	Percentage of frost days within a season (for seasons with tmean > 0 °C).	% of days	GS, SP, FA	800 m
GDD	Cumulative growing degree-days with base of 0, 4 or 5°C. Sum of tmean-base for all days tmean > base.	°C days	GS	800 m
GSL	Length of the growing season. Snow-free period where tmean ≥ 4 °C.	Days	Annual	800 m
Permafrost	Modelled near surface (≤ 1m) permafrost.	Probability	Annual	90 m
Ppt	Daily precipitation totals summed over the respective time period.	mm	Annual, GS, SP, FA, WI	800 m
Snow delay	Period between first daily tmean > 4 °C and first snow-free day.	Days	Annual	4 km
Snowfree	Median first snow-free day of the year for the available period 2006–2019.	Day of year	Annual	4 km
SPL	Length of the spring season. Period between tmax > 0° C and tmean < 4° C.	Days	Annual	800 m
Tmax	Daily maxmimum air temp. averaged over the respective time period.	°C	Annual, GS, SP, FA, WI	800 m
Tmean	Daily mean air temp. averaged over the respective time period.	°C	Annual, GS, SP, FA, WI	800 m
TmeanPK	Mean daily growing season air temp. using Paulsen and Körner's (2014) 0.9°C base.	°C	GS	800 m
Tmin	Daily minimum air temp. averaged over the respective time period.	°C	Annual, GS, SP, FA, WI	800 m
WIL	Length of the winter season. Period where tmax < 0°C.	Days	Annual	800 m
Wind	Daily mean wind speed averaged over the respective time period.	$m s^{-1}$	Annual, GS, SP, FA, WI	4 km

observed daily air temperature thresholds for xylogenesis (Rossi et al. 2008, Li et al. 2017) and the other using the 0.9°C base of Paulsen and Körner (2014) for direct comparison with their global analysis. Without appropriate soil moisture data, we did not subtract days from growing seasons to account for drought stress, which previous research indicates may be rare in mature white spruce across the Brooks Range (Brownlee et al. 2016). Mean GSAT was computed as the mean of all days during growing seasons, then extracted along all 12 400 km of our treelines with pixel values equal to treeline presence (response variable value = 1).

Model building and variable selection – which variables are most predictive of treeline presence?

Our sample dataset included 41 environmental variables with 61 441 observations, which we randomly split (50/50) into training (for model building) and validation (to assess model performance) datasets. Many variables related complexly with treeline presence (Supporting information). To accommodate these relationships, we used binomial generalized additive models (GAMs) to model treeline presence (mgcv package in R; Wood 2004, 2011). We reduced the variable set to the most ecologically relevant variables by sequentially choosing variables in order of importance using Akaike's information criterion (AIC) in univariate logistic GAMs (lowest AIC value = highest rank; model fits shown in Supporting information) while minimizing pairwise correlations (Spearman's correlation coefficient > |0.7|; the 'select07' method in Dormann et al. 2013). To reduce overfitting, we imposed smooth response curves by constraining the number of basis dimensions (k=4) for each term and applying an additional global penalty that lowers the effective sample size (gamma = 10).

With the resulting 14 ecologically meaningful, but minimally collinear, variables, we built a single GAM with all variables in the list. We then sequentially removed environmental variables that had pairwise concurvity (a nonlinear analog of collinearity) > 0.5 with any of the other variables based on the conservative 'worst-case concurvity' metric (Wood 2017). This process was repeated until the final model had pairwise concurvity ≤ 0.5 between all variables. Rather than relying on p-values (nearly all terms were significant due to large sample size), we conducted final variable selection by including a global penalty to smooth terms in the GAM which identifies weak variables by reducing their coefficients towards 0 (Marra and Wood 2011, Wood 2017). The final model fits to remaining variables were further refined by adjusting the number of basis dimensions (max k=10) for each smooth term and controlling the effective sample size.

We validated our final model by predicting treeline presence using the validation dataset and computing AUC as an absolute measure of performance. We checked for the influence of spatial autocorrelation on results (Dormann et al. 2007) by refitting a GAM with a residual autocovariate term (Crase et al. 2014) using the set of predictor variables identified after the select07 and concurvity exclusion processes. We

also fitted GAMs with spatial coordinates terms to examine if spatial autocorrelation could be accounted for in this way. We further validated our GAM results and variable rankings with a random forest model (randomForest package; Liaw and Wiener 2002). Variable ranking in the random forest was determined using permutation importance, a metric of increase in classification error resulting from the removal of each variable. After the model building process, we used the resulting GAM to construct a map of treeline probability over northern Alaska. Finally, to better understand how general climatic attributes (rather than specific variables) are associated with treelines, we also ran a principal components (PC) analysis on our suite of environmental variables and built another GAM predicting treeline presence from the PC axes.

Results

Testing the 6-7°C isotherm associated with the GLH

Mean GSAT at our treelines was not centered on 6–7°C and was almost universally warmer (Fig. 2). Using the 4°C base, all treeline pixels had mean GSAT warmer than 6.4°C (range: 7.1–11.2°C, mean: 9.3°C, median: 9.2°C; Fig. 3). For Paulsen and Körner's (2014) 0.9°C base, 99.99% of treeline pixels were warmer than 6.4°C (range: 6.2–10.6°C, mean: 8.5°C, median: 8.5°C; Fig. 2). For an inclusive comparison, we also considered the 6.7 ± 0.8°C (i.e. 5.9–7.5°C) isotherm reported by Körner and Paulsen (2004). For the 4°C base, only 0.02% (5 pixels) of treelines were below 7.5°C. With the 0.9°C base, 4.7% (1224 of 26 209 pixels) of treelines were below 7.5°C (Fig. 2). When mapped, the 6.7 ± 0.8°C isotherm occurs primarily along the northern coast, northern Brooks Range foothills and high in the Brooks Range – locations far beyond the majority of observed treelines (Fig. 3).

Which variables are most predictive of treeline presence?

The four most predictive variables of treeline presence in a univariate context were metrics of GSAT, with cumulative growing degree-days (4°C base; GDD4) being the most predictive (23.2% deviance explained=d.e.), followed by the two other calculations of growing degree-days and July mean air temperature (Table 2). The least predictive metrics of growing season warmth were air temperature means (GS_TmeanPK with 0.9°C base: 19.7% d.e., GS_Tmean with 4°C base: 20.0% d.e.), minimum (GS_Tmin: 14.3% d.e.) and maximum (GS_Tmax: 12.0% d.e.; Table 2). Annual maximum air temperature, growing season length and winter season length ranked similarly to mean GSAT (~20% d.e.). Overall, there were often small differences in AIC values and deviance explained between adjacently ranked univariate models (Table 2).

The final GAM included three predictors: GDD4, near-surface permafrost probability and growing season total precipitation (GS_Ppt; Supporting information, Fig. 4).

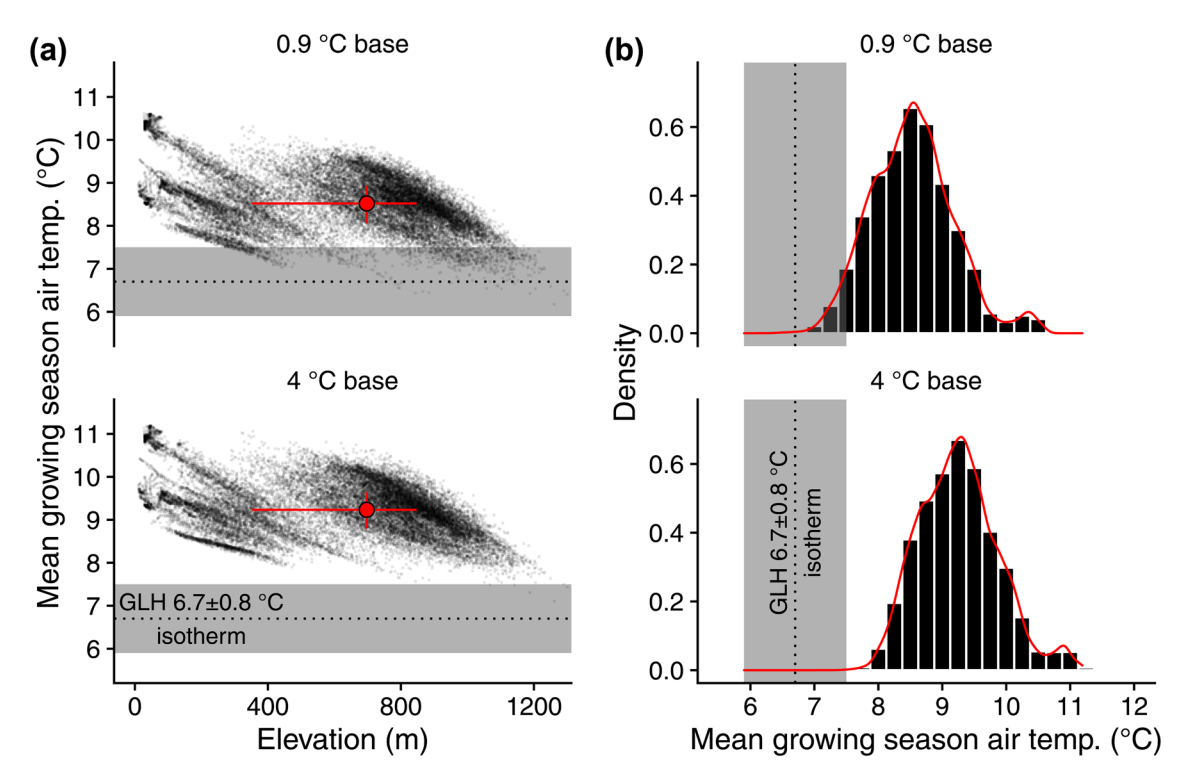


Figure 2. Disagreement between two metrics of mean growing season air temperature in northern Alaska and the $6.7 \pm 0.8^{\circ}$ C isotherm associated with the growth limitation hypothesis. Data were extracted for all treeline pixels identified in this study (n = 26 209 pixels; 12 400 km in total length). (a) Scatter plots of treeline mean growing season air temp. versus elevation. Red points and lines represent medians with 25 and 75% quantiles. (b) Relative distribution of treeline points across the range of mean growing season air temp. in 0.25° C bins. In both (a) and (b), top panels show growing season means calculated with the 0.9° C base used by Paulsen and Körner (2014). Bottom panels show growing season means calculated with a seasonal base temperature of 4° C informed by thermal limits of xylogenesis (Rossi et al. 2008, Li et al. 2017). The gray bars delineate the $6.7 \pm 0.8^{\circ}$ C isothem. Overlap with the 4° C base was 0.02% of treelines, with 0.9° C overlap was 4.7% of treelines.

This model explained 32.5% of the deviance in the training dataset with AUC=0.89 on the validation dataset, reflecting good overall model performance. Model residuals contained spatial autocorrelation (Moran's I=0.22 for 3×3 pixel neighbourhoods), but accounting for this with a residual autocovariate term did not change the order of variable importance (Supporting information). Including a spatial coordinates term did not affect residual autocorrelation. The random forest model also ranked predictors in the same order of importance as the GAM, with GDD4, permafrost probability and GS_Ppt as the top three (Supporting information). In the final GAM model, GDD4 and GS_Ppt showed clear optimums associated with treeline presence, with peaks near 650 growing degree-days and 80 mm of precipitation, respectively (Fig. 4). Lower GDD4 values reduced the probability of treeline at the higher elevations of the Brooks Range and along the northern coast (corresponding to <400 degreedays; Supporting information). The additional inflections in the GDD4 response reflect clusters of treelines near 450 and 850 growing degree-days. The low values occurred at treelines in the western and eastern Brooks Range and the highest values occurred primarily at low elevation treelines near the village of Ambler (Supporting information; Fig. 1 for location). Permafrost probability had a distinctive two-peaked pattern,

with most treelines clustered around 30% probability (Brooks Range and mountains south) and a secondary cluster above 75% probability (western low elevation treelines) (Fig. 4; Supporting information). GS_Ppt had a smaller influence on treeline presence (Supporting information, Fig. 4), with most treelines occurring at intermediate levels of GS_Ppt centered over the Brooks Range and mountains south (Supporting information).

Our best principal components GAM included PC1, PC2 and PC4 as predictors of treeline presence (Supporting information). PC3 and PC5 had weak effects and were dropped from the model. The results largely agree with the specificvariable GAM and provide further insight into the interrelated environmental factors associated with treeline. Lower PC1 values indicate warmer growing seasons, while high values represent longer winters, warmer, but windier, springs, windier growing seasons and later snow-free dates. Low PC2 values represent higher permafrost probability and greater frost occurrence, while high values represent warmer winters and increased precipitation. PC4 was lower for longer fall seasons, greater spring frost occurrence and windier winters. Larger PC4 values reflect greater delay in the start of growing seasons due to persistent snowpack and warmer spring and fall air temperatures. The PCA GAM achieved slightly

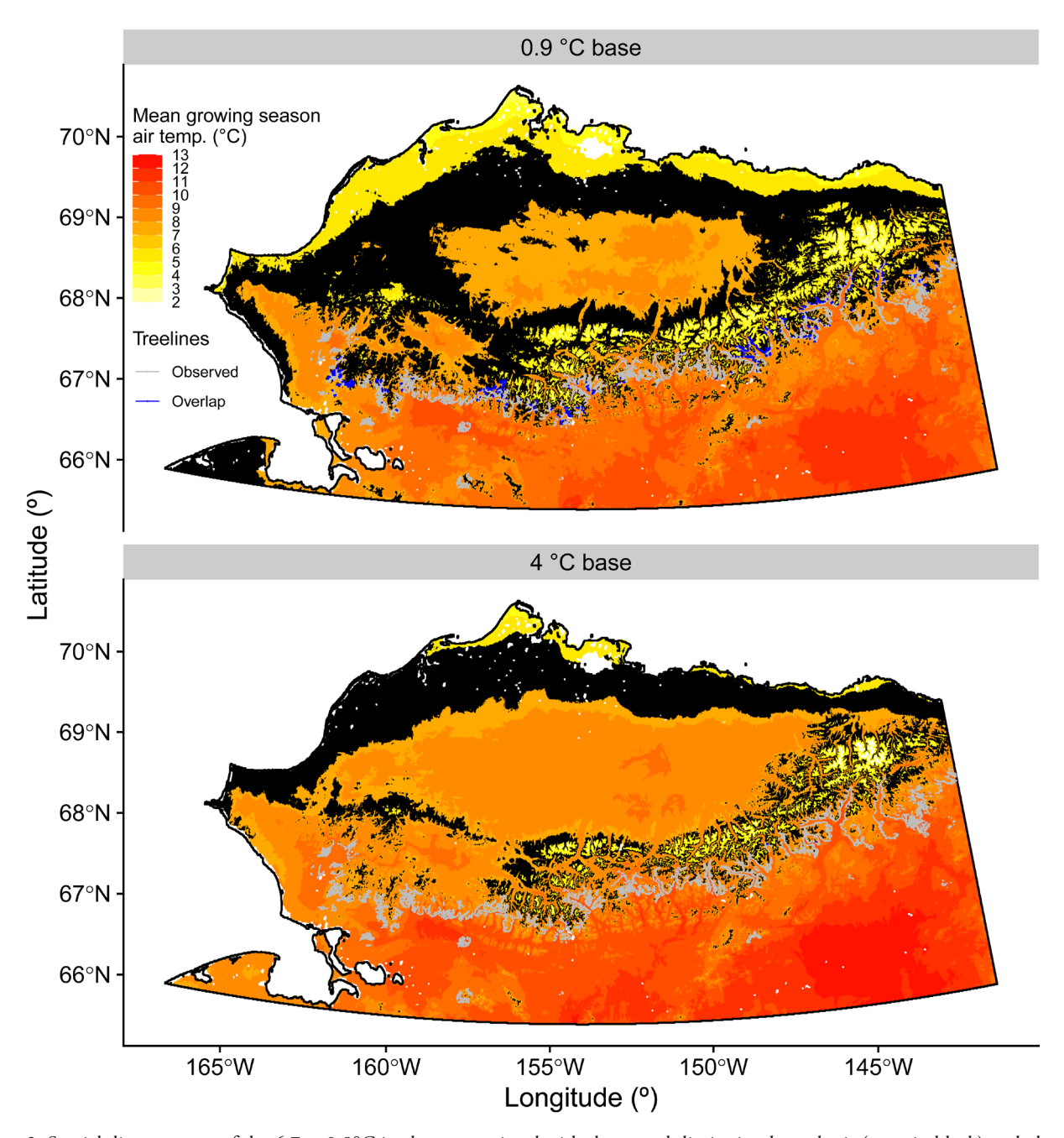


Figure 3. Spatial disagreement of the $6.7\pm0.8^{\circ}\text{C}$ isotherm associated with the growth limitation hypothesis (areas in black) and observed treelines (grey lines) over northern Alaska. Areas of overlap are highlighted in blue (4.7% of treelines in the top panel, 0.02% in the bottom panel). The top panel shows mean growing season air temperatures calculated with a base temperature of 0.9°C used by Paulsen and Körner (2014). Bottom panel shows growing season means calculated with a 4°C base informed by thermal limits of xylogenesis (Rossi et al. 2008, Li et al. 2017). Both metrics of growing season air temperature are derived from 1981 to 2010 normals.

lower AIC than the specific-variable GAM (16751 versus 16695) but did not improve prediction accuracy (AUC 0.88 versus 0.89) or deviance explained (32.3% versus 32.5%). Therefore, we used the specific-variable GAM for mapping predictions of treeline presence.

Mapping treeline predictions over northern Alaska

Mapped predicted treeline presence generally agreed well with observed treelines (Fig. 5). However, the model estimated

treelines in the central and western Brooks Range more accurately than in the eastern part of the range. Additionally, lowland treelines in non-mountainous terrain were poorly predicted. The model predicted treeline presence in several areas beyond and generally north of our observed treelines, most notably in the extreme western extent of the Brooks Range (De Long Mountains), the Wulik and Kivalina watersheds and the upper Noatak River Basin. The model also indicated non-negligible probabilities of treeline (<0.2) across a broad area of current tundra in the Colville River drainage

Table 2. Environmental variable rankings based on univariate logistic generalized additive models predicting treeline presence in northern Alaska. Table 1 for a key to variable names. Ranks are based on model AIC values.

Variable	AIC	Deviance explained	
GDD4	18 947.5	23.2	
GDD0	18 995.9	23.0	
GDD5	19 001.8	23.0	
July_Tmean	19 670.7	20.3	
AN_Tmax	19 738.3	20.0	
GS_Tmean	19 746.1	20.0	
GSL	19 752.7	20.0	
WIL	19 770.2	19.9	
GS_TmeanPK	19 823.7	19.7	
Snowfree	20 361.7	17.5	
GS_Tmin	21 158.8	14.3	
AN_Tmean	21 405.5	13.3	
GS_FrostRisk	21 452.4	13.1	
SP_Wind	21 467.1	13.0	
AN_Tmin	21 616.7	12.4	
GS_Tmax	21 724.0	12.0	
GS_Ppt	21 747.4	11.9	
FAL	21 905.6	11.3	
FA_Wind	22 141.1	10.3	
WI_Tmax	22 141.3	10.3	
GS_Wind	22 157.5	10.2	
WI_Tmean	22 198.6	10.1	
AN_Ppt	22 295.6	9.7	
SP_Ppt	22 303.2	9.6	
WI_Tmin	22 402.9	9.2	
WI_Ppt	22 615.8	8.4	
GS_snowdelay_PK	22 716.3	8.0	
Permafrost	22 771.1	7.7	
GS_snowdelay	22 892.1	7.3	
AN_Wind	22 950.5	7.0	
SP_FrostRisk	22 954.5	7.0	
FA_Ppt	22 964.1	7.0	
SP_Tmin	22 965.4	7.0	
SP_Tmean	23 293.3	5.6	
WI_Wind	23 596.1	4.4	
SPL	23 729.5	3.9	
FA_Tmean	23 780.0	3.7	
FA_Tmin	24 046.5	2.6	
FA_Tmax	24 128.9	2.2	
FA_FrostRisk	24 334.9	1.4	
SP_Tmax	24 363.1	1.3	

of the north Slope. In the eastern Brooks Range, the model predicted treelines in the Kongakut River valley (Fig. 5; Fig. 1 for locations).

Discussion

Identifying the climatic variables associated with northern treelines is an important aspect of predicting responses of arctic and subarctic ecosystems to climate change and their feedbacks to the climate system. Treelines are generally thought to be controlled by GSAT, and other environmental variables are rarely considered over a broad scale. Our modelling approach allowed consideration of the relationship of

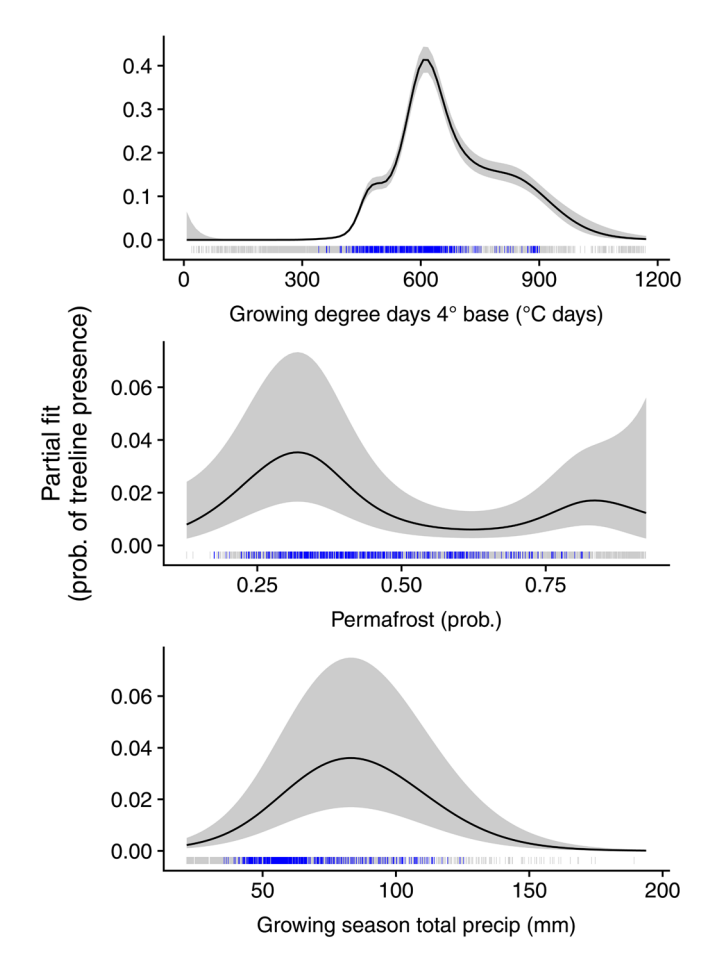


Figure 4. Partial response plots from a binomial logistic generalized additive model predicting treeline presence as a function of cumulative growing degree-days (4°C base), near surface (≤ 1 m) permafrost probability and growing season total precipitation. Response curves for each variable show the predicted response when the other variables are held at their mean values. Confidence intervals (gray bands) show \pm 2 SE associated with each smooth term, plus the uncertainty associated with the overall model fit. Hash mark 'rugs' show distribution of pixels containing treelines (blue) over pixels without treelines (gray).

treeline with several environmental factors across northern Alaska. We interpreted our results with respect to the GLH: 1) mean GSAT at treelines in northern Alaska is consistently far warmer than the 6-7°C isotherm associated with the GLH and 2) treeline was best predicted by a model containing GDD4, permafrost probability and GS_Ppt. If GSAT was the primary limiting factor for treelines in our study area, we would see consistency between observed treelines and the GLH isotherm. Instead, our results indicate that while there is a substantial role of growing season warmth in predicting treelines, we reject the growth limitation hypothesis as the direct causal mechanism of treelines in Arctic Alaska. Our model predicted non-zero treeline probability in several areas that are not currently known to contain trees but are near observed treelines. These areas present low climatic barriers and may be future locations of treeline advance.

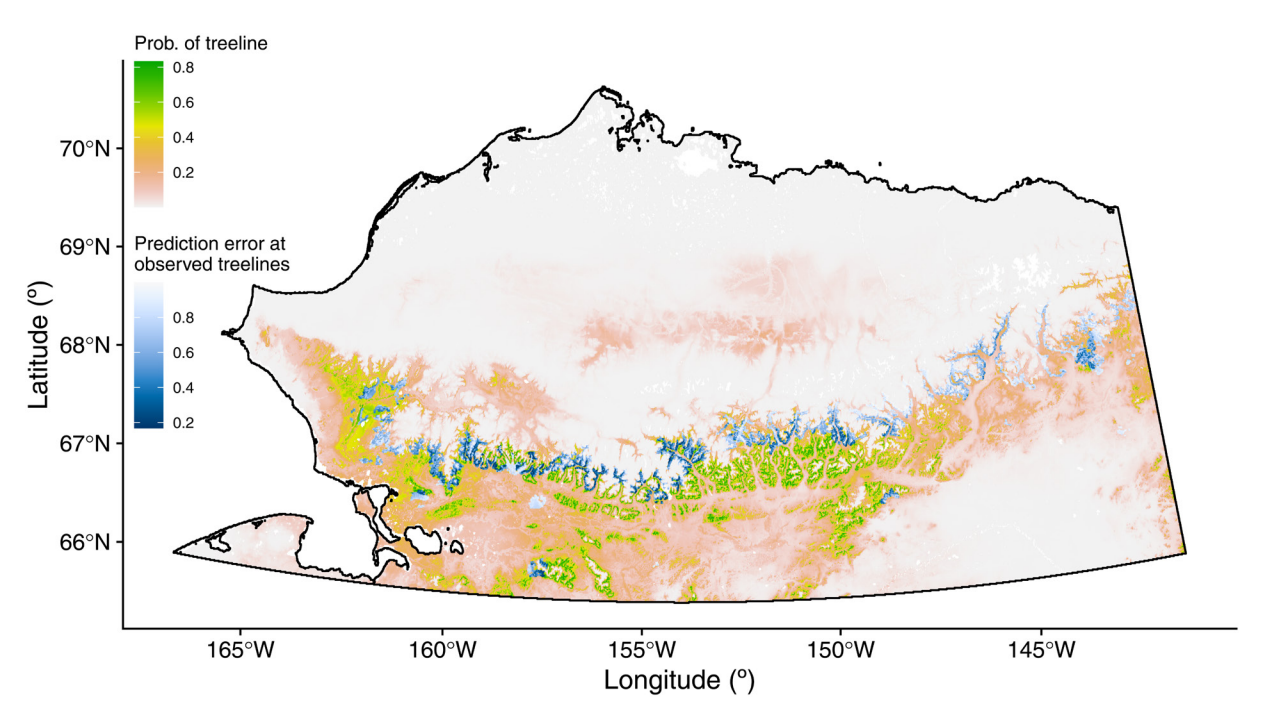


Figure 5. Map of predicted treeline presence in northern Alaska (expressed as probabilities) showing generally good agreement with many observed treelines. Areas beyond the current treeline highlighted by the model may indicate likely locations of treeline expansion. Predictions derive from a logistic generalized additive model with cumulative growing degree-days (4°C base), near surface (≤1 m) permafrost probability and growing season total precipitation as predictors. Prediction error at observed treeline points (1-predicted probability) is shown with blue shading.

Treelines that are warmer than the 6-7°C mean GSAT isotherm (Millar et al. 2020) may indicate that growth limitation due to cold GSAT is not the dominant factor determining those treelines or that it is codominant with other factors. It is also possible that treeline positions simply lag behind warming or that Alaska's northern treelines display nonequilibrium behaviour (sensu Scheffer et al. 2012) and have not yet reached a critical mean GSAT. However, our results cannot be fully explained by lagged responses following release from direct physiological limitation by GSAT. First, our climate data account for >1 decade of lag (1981– 2010 climate normals with 2006-2019 imagery). Second, the trends in May-September mean air temperature across northern Alaska were −0.03°C·decade⁻¹ for 1901–1950 and 0.28°C·decade⁻¹ for 1951–2010 (Supporting information). At these rates, our 8.5 and 9.3°C GSAT means for 1981-2010 (midpoint=1995) were ~7.2 and ~8°C for the relatively static 1901–1950 period (data from Scenarios Network for Alaska and Arctic Planning, https://uaf-snap.org/get- data/>). A majority of our treelines have thus been warmer than 6-7°C for at least 120 years. Instead of direct control by GSAT, warm growing seasons, the low explained deviance of our model and the combination of variables in the model may indicate the importance of missing or inadequately characterized variables in our analysis, such as soil temperature, snow depth or wind. It is also possible that our results reflect the roles of non-climatic factors, like tree demography, dispersal, competition, herbivory, disturbance (e.g. bark beetles, fire) and their interactions. Warmer GSAT than expected under

the GLH likely indicates that 'regionally variable modulatory forces' – hypothesized by Körner (1998) to secondarily augment the fundamental importance of GSAT as predictors of treeline – are the rule, rather than the exception at Alaska's northern treelines.

The strong influence of GDD4 in our model could reflect a primary role of GSAT in limiting tree growth, reproduction, germination or survival at treeline (i.e. support of the GLH). GDD was found to be an important correlate of tree and seedling establishment - the prerequisites of treeline advance - at an advancing treeline in southwestern Alaska (Miller et al. 2017). However, our observation of GSATs warmer than the GLH isotherm indicate that direct physiological limitation from low GSAT is unlikely to explain the position of treelines in northern Alaska. Additionally, we found that winter length was almost as influential as metrics of growing season warmth on the PC1 axis (Supporting information). Although this association could be arithmetic (longer winters will generally accompany shorter, cooler summers), the importance of winter for tree growth and treeline position has been recognized elsewhere (Hagedorn et al. 2014, Harsch et al. 2014, Sullivan et al. 2015, Renard et al. 2016). Thus, we interpret these results as indicating that mechanisms relating to both growing season warmth and winter season length are important predictors of treeline in northern Alaska. One such mechanism may be soil temperature and its related soil processes, which have previously been hypothesized as the primary or co-dominant limiting factors of treelines in northern Alaska (Sullivan et al. 2015).

While the effects of soil temperature and related processes are likely not fully captured in our analysis, the predictor variables in our final model (GDD4, permafrost probability and GS Ppt) together may act as surrogates for soil temperature. The temperature of soil above permafrost is correlated with air temperature at a coarse scale, but it is strongly affected by other factors and processes such as vegetation, soil properties and conditions (e.g. organic layer thickness, moisture and texture), snow accumulation, conductive exchange with snowmelt water and latent heat exchange from phase changes of water in the soil (Hinkel et al. 2001). Summer soil temperature is also typically much cooler than air temperature near boreal treelines (Sullivan et al. 2015, Ellison et al. 2019), which could account for the mismatch between our treelines and the GLH isotherm. The temporal lag associated with warming soils could account for apparent nonequilibrium behaviour with respect to air temperature and treeline position. The inclusion of precipitation in our final model could reflect an influence of longitudinal moisture gradients on tree growth at treeline (Wilmking and Juday 2005) but could also further reflect the importance of winter climate or the role of soil water on soil temperature.

Cold soils can directly affect root growth (Tryon and Chapin 1983) and can also indirectly affect growth by negatively affecting water transport (Running and Reid 1980) and nutrient absorption (Stevens and Fox 1991, Weih and Karlsson 2002). Although trees are dormant through winter, winter soil temperature affects soil microbial activity (Sturm et al. 2005, Sullivan et al. 2020) and can indirectly affect trees by limiting microbial nutrient mineralization (Nadelhoffer et al. 1991, Dawes et al. 2017), which ultimately restricts nutrient availability in the growing season (Sveinbjörnsson 2000, Sullivan et al. 2015). An analysis of factors affecting vegetation distributions in northwest Alaska found that white spruce cover was associated with greater active layer and water table depths than unforested areas, indicating the importance of drainage (Jorgenson et al. 2009). These soil properties can in turn be affected by topography, with the warmest, bestdrained soils occurring on south-facing slopes. Our model performed relatively poorly in predicting current treelines in the eastern Brooks Range, a region with the highest elevation treelines, the greatest differences between air and soil temperature, and lower soil nutrient availability than elsewhere in the Brooks Range (Ellison et al. 2019). However, climate station coverage is limited in this area. Although the soil temperature interpretation is plausible, our model only explained 32.5% of the deviance in the dataset. Inaccuracies in gridded climate data probably limited explanatory power, although it seems likely that we lacked important climatic predictor variables, or that treeline positions in our study region are dependent on non-climatic factors not easily characterized at broad scales.

Non-climatic factors, such as population and community dynamics and disturbance, are known to be important in determining treeline movement. Dispersal of seeds can be more important than abiotic constraints in determining establishment in habitats near current treelines (Stueve et al.

2011). Factors that limit successful dispersal - seeds reaching suitable microsites and establishment of individuals in those sites - can cause lags in tree population expansion behind climatic conditions (Johnstone and Chapin 2003). Herbivory of seedlings during peaks in snowshoe hare Lepus americanus abundance can prevent spruce establishment near treelines in interior Alaska and could substantially slow treeline advance in areas with favourable hare habitat (e.g. tall shrubs; Olnes et al. 2017). Additionally, mortality of mature trees reduces seed sources. Porcupine Erethizon dorsatus feeding on the cambium of *P. glauca* can kill mature trees (Payette 2007), while spruce bark beetles Dendroctonus rufipennis can induce widespread mortality. Spruce bark beetle outbreaks have historically been infrequent in northern Alaska, but warming winters may increase their frequency (Berg et al. 2006). Similarly, while wildfire has historically been rare near the northern treeline in Alaska, by the century's end, the frequency of lightning strikes at treeline is projected to match rates currently experienced in interior Alaska (Chen et al. 2021). It seems clear that these non-climatic factors will affect the character of treeline movement in complex ways as the climate and Arctic ecosystems continue to change.

Although extensive field-based research is needed to make fine-scale predictions of how treelines may shift (and how rapidly) in coming decades, our model predictions may broadly indicate regions that present low climatic barriers to treeline advance. In northwest Alaska in particular, our model identified extensive areas that may be able to support trees beyond currently known treelines. Previous research identified the Brooks Range as a major geographic barrier to northward treeline advance, possibly delaying warminginduced treeline advance by 1000+ years with 'low barrier' areas in the upper Noatak River Basin (Rupp et al. 2001). Agreement between our predictions and those of Rupp et al. (2001) indicates this region is a potential front of treeline advance in the near future, although advance will be substantially modified by non-climatic factors. Near-surface permafrost is rapidly thawing in northwest Alaska, with active layer thickness projected to more than double in the next 35 years (Batir et al. 2017). Treeline advance related to permafrost thaw has been observed in western Alaska (Lloyd et al. 2003) and may be especially important in river floodplains where deep active layers border areas of tundra with shallow active layers, forming abrupt treelines (Epstein et al. 2004). Changes in boreal forest extent will have important implications for wildlife movement and distribution patterns (Mallory and Boyce 2018, Zhou et al. 2020) and human subsistence use (Brinkman et al. 2016). Increasing tree coverage in the Arctic is also expected to amplify climate warming through changes in surface albedo and carbon cycling (Chapin et al. 2005). Shifting boreal treelines are thus expected to be both a cause and a consequence of continued rapid warming in the Arctic.

Acknowledgements – Any use of trade, firm or product names is for descriptive purposes only and does not imply endorsement by the U.S. Government.

Funding – This project was funded by National Science Foundation (NSF) awards OPP-1748849 to PFS, OPP-1748773 to RJD and OPP-1748847 to REH. CTM was supported by NSF award OPP-1748849. NJP acknowledges funding support from the USGS Land Change Science Program.

Author contributions

Colin Maher: Conceptualization (equal); Data curation (lead); Formal analysis (lead); Investigation (lead); Methodology (lead); Visualization (lead); Writing – original draft (lead); Writing – review and editing (lead). Roman Dial: Conceptualization (equal); Formal analysis (equal); Funding acquisition (equal); Methodology (equal); Supervision (equal); Visualization (supporting); Writing – original draft (supporting); Writing - review and editing (equal). Neal Pastick: Formal analysis (supporting); Writing – original draft (equal); Writing - review and editing (equal). Rebecca Hewitt: Formal analysis (supporting); Funding acquisition (equal); Supervision (equal); Writing – original draft (equal); Writing - review and editing (equal). **Torre Jorgenson**: Writing original draft (equal); Writing - review and editing (equal). Patrick Sullivan: Conceptualization (equal); Formal analysis (equal); Funding acquisition (equal); Methodology (equal); Supervision (equal); Visualization (supporting); Writing – original draft (equal); Writing – review and editing (equal).

Transparent Peer Review

The peer review history for this article is available at https://publons.com/publon/10.1111/ecog.05597.

Data availability statement

Data and analysis code is archived at the National Science Foundation's Arctic Data Center (primary data and analysis: https://doi.org/10.18739/A2SQ8QJ7T; mapping seasonal climate variables: https://doi.org/10.18739/A2280506H) (Maher et al. 2021).

References

- Abatzoglou, J. T. et al. 2018. TerraClimate, a high-resolution global dataset of monthly climate and climatic water balance from 1958 to 2015. Sci. Data 5: 1–12.
- Bader, M. Y. et al. 2020. A global framework for linking alpinetreeline ecotone patterns to underlying processes. – Ecography 44: 265–292.
- Batir, J. F. et al. 2017. Ten years of measurements and modeling of soil temperature changes and their effects on permafrost in Northwestern Alaska. Global Planet. Change 148: 55–71.
- Berg, E. E. et al. 2006. Spruce beetle outbreaks on the Kenai Peninsula, Alaska and Kluane National Park and Reserve, Yukon Territory: relationship to summer temperatures and regional differences in disturbance regimes. For. Ecol. Manage, 227: 219–232.
- Bergstra, J. and Bengio, Y. 2012. Random search for hyper-parameter optimization. J. Mach. Learn. Res. 13: 281–305.
- Breiman, L. 2001. Random forests. Mach. Learn. 45: 5-32.

- Brinkman, T. J. et al. 2016. Arctic communities perceive climate impacts on access as a critical challenge to availability of subsistence resources. Clim. Change 139: 413–427.
- Brownlee, A. H. et al. 2016. Drought-induced stomatal closure probably cannot explain divergent white spruce growth in the Brooks Range, Alaska, USA. Ecology 97: 145–159.
- Chapin III, F. S. et al. 2005. Role of land-surface changes in arctic summer warming. Science 310: 657–660.
- Chen, Y. et al. 2021. Future increases in Arctic lightning and fire risk for permafrost carbon. Nat. Clim. Change 11: 404–410.
- Crase, B. et al. 2014. Incorporating spatial autocorrelation into species distribution models alters forecasts of climate-mediated range shifts. Global Chang. Biol. 20: 2566–2579.
- Daly, C. et al. 2008. Physiographically sensitive mapping of climatological temperature and precipitation across the conterminous United States. Int. J. Climatol. 28: 2031–2064.
- Daubenmire, R. 1954. Alpine timberlines in the Americas and their interpretation. Butl. Univ. Bot. Stud. 11: 119–136.
- Dawes, M. A. et al. 2017. Soil warming opens the nitrogen cycle at the alpine treeline. Global Change Biol. 23: 421–434.
- Dial, R. J. et al. 2016. Shrubline but not treeline advance matches climate velocity in montane ecosystems of south-central Alaska.
 Global Change Biol. 22: 1841–1856.
- Dormann, C. F. et al. 2007. Methods to account for spatial autocorrelation in the analysis of species distributional data: a review. Ecography 30: 609–628.
- Dormann, C. F. et al. 2013. Collinearity: a review of methods to deal with it and a simulation study evaluating their performance. Ecography 36: 27–46.
- Ellison, S. B. Z. et al. 2019. Poor nutrition as a potential cause of divergent tree growth near the Arctic treeline in northern Alaska. Ecology 100: 1–18.
- Epstein, H. E. et al. 2004. The nature of spatial transitions in the Arctic. J. Biogeogr. 31: 1917–1933.
- Gannett, H. 1899. The timber line. J. Am. Geogr. Soc. New York 31: 118–122.
- Gorelick, N. et al. 2017. Google Earth Engine: planetary-scale geospatial analysis for everyone. Remote Sens. Environ. 202: 18–27.
- Hagedorn, F. et al. 2014. Treeline advances along the Urals mountain range driven by improved winter conditions? Global Change Biol. 20: 3530–3543.
- Hall, D. K. et al. 2016. MODIS/Terra Snow Cover Daily L3 Global 500m Grid Ver. 6. – NASA National Snow and Ice Data Center Distributed Active Archive Center, Boulder, Colorado, USA.
- Harsch, M. A. et al. 2009. Are treelines advancing? A global metaanalysis of treeline response to climate warming. – Ecol. Lett. 12: 1040–1049.
- Harsch, M. A. et al. 2014. Winter climate limits subantarctic low forest growth and establishment. PLoS One 9: e93241.
- Hijmans, Ř. J. 2021. raster: geographic data analysis and modeling. R package ver. 3.4-13. https://cran.r-project.org/web/packages/raster/index.html.
- Hijmans, R. J. et al. 2005. Very high resolution interpolated climate surfaces for global land areas. Int. J. Climatol. 25: 1965–1978.
- Hinkel, K. M. et al. 2001. Patterns of soil temperature and moisture in the active layer and upper permafrost at Barrow, Alaska: 1993–1999. Global Planet. Change 29: 293–309.
- Holtmeier, F. and Broll, G. 2020. Treeline research from the roots of the past to present time. A review. Forests 11: 1–31.

- Johnstone, J. F. and Chapin, F. S. 2003. Non-equilibrium succession dynamics indicate continued northern migration of lodge-pole pine. Global Change Biol. 9: 1401–1409.
- Jorgenson, M. T. and Meidinger, D. 2015. The Alaska-Yukon region of the circumboreal vegetation map (CBVM). – CAFF strategies series report. Conservation of Arctic flora and fauna, Akureyri, Iceland.
- Jorgenson, M. T. et al. 2009. An ecological land survey and land-cover map of the Arctic network, National Park Service, Ft Collins, CO. Natural Resources Technical Report NPS/ARCN/NRTR 2009/270: 307.
- Körner, C. 1998. A re-assessment of high elevation treeline positions and their explanation. Oecologia 115: 445–459.
- Körner, C. 2012. Alpine treelines: functional ecology of the global high elevation tree limits. Springer.
- Körner, C. and Paulsen, J. 2004. A world-wide study of high altitude treeline temperatures. J. Biogeogr. 31: 713–732.
- Li, X. et al. 2017. Critical minimum temperature limits xylogenesis and maintains treelines on the southeastern Tibetan Plateau. Sci. Bull. 62: 804–812.
- Liaw, A. and Wiener, M. 2002. Classification and regression by randomForest. R News 2: 18–22.
- Lloyd, A. H. et al. 2003. Patterns and dynamics of treeline advance on the Seward Peninsula, Alaska. J. Geophys. Res. 108: 8161.
- Maher, C. T. et al. 2021. Data from: The climate envelope of Alaska's northern treelines: implications for controlling factors and future treeline advance. National Science Foundation's Arctic Data Center, https://doi.org/10.18739/A2SQ8QJ7T, https://doi.org/10.18739/A2SQ8QJ7T,
- Mallory, C. D. and Boyce, M. S. 2018. Observed and predicted effects of climate change on Arctic caribou and reindeer. Environ. Rev. 26: 13–25.
- Man, R. and Lu, P. 2010. Effects of thermal model and base temperature on estimates of thermal time to bud break in white spruce seedlings. Can. J. For. Res. 40: 1815–1820.
- Marra, G. and Wood, S. N. 2011. Practical variable selection for generalized additive models. Comput. Stat. Data Anal. 55: 2372–2387.
- Millar, C. I. et al. 2020. From treeline to species line: thermal patterns and growth relationships across the krummholz zone of whitebark pine, Sierra Nevada, California, USA. Arctic Antarct. Alp. Res. 52: 390–407.
- Miller, A. É. et al. 2017. Warming drives a front of white spruce establishment near western treeline, Alaska. Global Change Biol. 23: 5509–5522.
- Nadelhoffer, K. J. et al. 1991. Effects of temperature and substrate quality on element mineralization in six Arctic soils. Ecology 72: 242–253.
- Olnes, J. et al. 2017. Can snowshoe hares control treeline expansions? Ecology 98: 2506–2512.
- Pastick, N. J. et al. 2015. Distribution of near-surface permafrost in Alaska: estimates of present and future conditions. – Remote Sens. Environ. 168: 301–315.
- Pastick, N. J. et al. 2017. Historical and projected trends in landscape drivers affecting carbon dynamics in Alaska. – Ecol. Appl. 27: 1383–1402.
- Paulsen, J. and Körner, C. 2014. A climate-based model to predict potential treeline position around the globe. Alp. Bot. 124: 1–12
- Payette, S. 2007. Contrasted dynamics of northern Labrador tree lines caused by climate change and migrational lag. – Ecology 88: 770–780.

- Pielke, R. A. and Vidale, P. L. 1995. The boreal forest and the polar front. J. Geophys. Res. 100: 755–758.
- Renard, S. M. et al. 2016. Winter conditions not summer temperature influence establishment of seedlings at white spruce alpine treeline in Eastern Quebec. J. Veg. Sci. 27: 29–39.
- Risser, P. G. 1995. The status of the science examining ecotones.

 Bioscience 45: 318–325.
- Romanovsky, V. E. and Osterkamp, T. E. 2000. Effects of unfrozen water on heat and mass transport processes in the active layer and permafrost. Permafr. Periglac. Process. 11: 219–239.
- Rossi, S. et al. 2008. Critical temperatures for xylogenesis in conifers of cold climates. Global Ecol. Biogeogr. 17: 696–707.
- Running, S. W. and Reid, C. P. 1980. Soil temperature influences on root resistance of *Pinus contorta* seedlings. Plant Physiol. 65: 635–640.
- Rupp, T. S. et al. 2001. Modeling the influence of topographic barriers on treeline advance at the forest-tundra ecotone in northwestern Alaska. Clim. Change 48: 399–416.
- Scheffer, M. et al. 2012. Anticipating critical transitions. Science 338: 344–348.
- Stevens, G. C. and Fox, J. F. 1991. The causes of treeline. Annu. Rev. Ecol. Syst. 22: 177–191.
- Stueve, K. M. et al. 2011. Spatial variability of biotic and abiotic tree establishment constraints across a treeline ecotone in the Alaska Range. Ecology 92: 496–506.
- Sturm, M. et al. 2005. Winter biological processes could help convert arctic tundra to shrubland. Bioscience 55: 17–26.
- Sullivan, P. F. et al. 2015. Evidence of soil nutrient availability as the proximate constraint on growth of treeline trees in northwest Alaska. Ecology 96: 716–727.
- Sullivan, P. F. et al. 2020. Labile carbon limits late winter microbial activity near Arctic treeline. Nat. Commun. 11: 4024.
- Sveinbjörnsson, B. 2000. North American and European treelines: external forces and internal processes controlling position. Ambio 29: 388–395.
- Tryon, P. R. and Chapin, F. S. I. 1983. Temperature control over rot growth and root biomass in taiga forest trees. Can. J. For. Res. 13: 827–833.
- Tuhkanen, S. 1993. Treeline in relation to climate, with special reference to oceanic areas. In: Alden, J. N. et al. (eds), Forest development in cold cimates. NATO ASI series (series A: life sciences). Vol. 244. Springer, Boston, MA, pp. 115–134.
- U.S. National Ice Center 2008. IMS daily Northern Hemisphere snow and ice analysis at 1 km, 4 km and 24 km resolutions, ver. 1 [4 km resolution]. – NSIDC Natl. Snow Ice Data Center, Boulder, Color. USA.
- Viereck, L. A. and Little, E. L. 2007. Alaska trees and shrubs. Univ. of Alaska Press.
- Weih, M. and Karlsson, P. S. 2002. Low winter soil temperature affects summertime nutrient uptake capacity and growth rate of mountain birch seedlings in the subarctic, Swedish Lapland. Arctic Antarct. Alp. Res. 34: 434–439.
- Wilmking, M. and Juday, G. P. 2005. Longitudinal variation of radial growth at Alaska's northern treeline recent changes and possible scenarios for the 21st century. Global Planet. Change 47: 282–300.
- Wilmking, M. et al. 2006. Effect of tree line advance on carbon storage in NW Alaska. J. Geophys. Res. Biogeosci. 111: 1–10.
- Wood, S. N. 2004. Stable and efficient multiple smoothing parameter estimation for generalized additive models. J. Am. Stat. Assoc. 99: 673–686.

- Wood, S. N. 2011. Fast stable restricted maximum likelihood and marginal likelihood estimation of semiparametric generalized linear models. I. R. Stat. Soc. 73: 3–36.
- linear models. J. R. Stat. Soc. 73: 3–36.
 Wood, S. N. 2017. Generalized additive models: an introduction with R. Chapman & Hall/CRC Press.
- Wylie, B. et al. 2016. Soil carbon and permafrost estimates and susceptibility in Alaska. In: Zhu, Z. and
- McGuire, A. D. (eds), Baseline and projected future carbon storage and greenhouse-gas fluxes in ecosystems of Alaska. U.S. Geological Survey, Reston, Virginia, USA, pp. 53–76.
- Zhou, J. et al. 2020. Enhanced shrub growth in the Arctic increases habitat connectivity for browsing herbivores. Global Change Biol. 26: 3809–3820.